Tuijin Jishu/Journal of Propulsion Technology
ISSN: 1001-4055
Vol. 44 No. 2 (2023)

The Wall Features of a Non-Uniform Tube affect the Peristaltic Motion of the Rabinowitsch Fluid Model

Dr. Uday Raj Singh[1], Uma Shanker[2]
[1]Professor, Department of Mathematics, C.L. Jain (P.G.) College, Firozabad, U.P. (India)
[2]Research Scholar, Department of Mathematics, C.L. Jain (P.G.) College, Firozabad, U.P. (India)
Affiliated to Dr. Bhimrao Ambedkar University, Agra

Abstract- The process known as peristaltic transfer is essential to the functioning of both physiological processes and peristaltic pumps. It has become abundantly evident that physiological fluids do not behave in the same way that Newtonian fluids do as a result of the progression of medical research. Therefore, selecting a suitable fluid model is of utmost importance if one wants to gain an understanding of the behaviour and characteristics of physiological fluids throughout the process of peristalsis. The Rabinowitsch fluid model with wall properties was utilised in this investigation to investigate the characteristics of peristaltic transport via a non-uniform tube while the tube was carrying a non-Newtonian fluid. A theoretical analysis that uses an approximation with a long wavelength and a low Reynolds number has been provided. In order to investigate the properties of the stream function, the velocity distributions and temperature distributions have been measured. The relevant numerical results to the effects of variables such as the Brickman number Br, the rigidity parameter e_1,, the stiffness parameter e_2, and the viscous damping force parameter e_3 are all connected to the underlying flow problem, and we have calculated these results. It has been demonstrated that non-Newtonian fluids and uneven tube walls are both capable of dramatically modifying these features.

Keywords: *Non-uniform Tube, Peristalsis, Rabinowitsch Fluid Model.*

1. Introduction-

The study of peristaltic flows has risen in prominence in recent decades due to the wide range of fields in which it finds utility, including everyday life, engineering, and industry. Peristaltic flow has many uses in engineering and industry, including the delivery of fuels and lubricants (mobilising oils) to moving parts of machines, the transport of pulps to the food industry, the transport of melts to the plastics and polymer industry, the transport of sanitary fluids and the transport of corrosive fluids in everyday life, and the delivery of medicine via the bile duct, the gastrointestinal tract, the female fallopian tube, and other medical injector devices. More information is available in reputable publications.

Because biological systems and their components are complex designs, mathematical modeling of these systems is a popular research area. Peristalsis is an important mechanism for moving biological fluids through various bodily organs of the body. Peristalsis is the movement of fluid in tubes caused by the contraction and expansion of the walls. Peristaltic flow analysis has become increasingly popular among biomechanics researchers over the past decades because it is useful in many areas of biomedical science and engineering. Food swallowing, chyme movement within the gastrointestinal tract, blood flow, and sperm movement within the efferent duct of the male reproductive system are examples of various applications of peristalsis in the human body. The Peristaltic Pump enables efficient transfer of a wide range of liquids with varying and complex rheological properties. The principle of pumping is called peristalsis. Channels within the system periodically and unconsciously contract and then relax or expand. As the pressure gradient increases, the liquid is propelled forward. In physiology, we see this type of pumping when food and fluids move through the digestive tract, when urine flows from the kidneys through the ureters into the bladder, when bile flows from the gallbladder into the duodenum, when sperm move through the male reproductive tract and the cervical drains, when eggs move through the fallopian tubes, and when

blood circulates through the capillaries. The study of peristalsis from a technical point of view began much later than physiological studies. Peristaltic pumps are used in industrial fluid machinery to transport products such as aggressive chemicals, high solids slurries and toxic liquids. Many medical devices such as roller pumps, hose pumps, peristaltic pumps, ginger pumps, heart-lung machines, blood pumping machines, dialysis machines, etc. are based on the principle of peristaltic motion. Kameswaran et al. (2013) studied homogeneous-heterogeneous reactions by studying the flow of nanofluids across contracting/stretching sheets. The leaves are placed in a porous medium saturated with copper- and silver-water nanoliquids. non-Newtonian fluids (Rabinowitsch fluid model) were included in the peristaltic flow in tube study by Singh and Singh (2014). Both velocity and pressure gradient problems were solved analytically. For homogeneous and heterogeneous processes in elastic peristaltic channels, we analyzed the Singh et al. (2017) Rabinowitsch liquid model. To better understand flow behavior in arterial vessels, Absi (2018) developed a new relationship between pressure and area. Goud and Reddy (2018) found that the velocity profile of a shear thickening fluid is a decreasing function of stiffness and stiffness parameters, and an increasing function of the viscous damping force parameter due to decreasing wall drag. Sarabana et al. (2018) studied the effect of heat transfer on the movement of a Rabinowicz fluid through a flexible-walled peristaltic conduit. Using various tube deformations, Nahar et al. (2019) studied the effects of Newtonian and non-Newtonian fluid flow using low- and high-shear thinning fluids, respectively.

Two-dimensional peristaltic flow of non-Newtonian fluids in magnetic fields was reported by Hasan et al. explained. (2019) in asymmetric porous channels. Imran et al. (2020) studied the effects of heterogeneous-homogeneous reactions and thermal radiation on his Rabinowitsch liquid model of peristaltic flow. Considering the different properties of liquids, Rajashekhar et al. (2020) obtained analytical conclusions about the unstable motion of liquids in the Rabinovitch potential. It was hypothesized that heterogeneous and homogenous chemical reactions occur when Rabinowicz liquids flow through inclined and heterogeneous channels. In a theoretical study, Yasodhara et al. (2020) studied the peristaltic motion of a non-Newtonian fluid in a horizontal tube with elastic walls. The effect of a radial magnetic field on the peristaltic motion of Casson fluid in a heterogeneous conduit was reported by Divya et al. Examined. (2021). The duct wall properties are taken into account. Moreover, the changing viscosity of the assumed liquid varies exponentially with channel width. Peristaltic movement of Eyring-Powell fluids through smooth and uneven channels was reported by Bhattacharyya et al. Examined. (2022). One of her research focuses is the relationship between wall flexibility and Joule heating. A simpler system can be realized by applying the long wavelength, low Reynolds number idea. Magneto-peristaltic flow of Casson fluid in a rotary-tilt system through asymmetric channels was reported by Hafez et al. Discussed. (2023). After obtaining the governing equations for the model, we make some simplifications (longer wavelengths, lower Reynolds number) so that we can approach it analytically.

2. Mathematical Formulation-

Think about how an incompressible, non-Newtonian fluid might move through a tube that was not completely uniform. Progressive sinusoidal wave trains travel at the speed c along the wall of the tube as they travel in a tube.

Wall geometry is expressed as

$$\bar{h} = b + m\bar{z} + asin\frac{2\pi}{\lambda}(\bar{z} - c\bar{t}) \quad (1)$$

where b is the inlet radius of the tube, m is a constant whose magnitude is proportional to the tube's length, $\bar{a}$ is the wave's amplitude, λ is the wavelength, c is the wave's propagation velocity, and $\bar{t}$ is the time it takes for the wave to travel through the tube.

For the one-dimensional Rabinowitsch fluid model, the following stress-strain relation is valid:

$$\bar{\tau}_{rz} + \kappa\bar{\tau}_{rz}{}^3 = \bar{\mu}\frac{d\bar{w}}{d\bar{r}} \quad (2)$$

where $\bar{\mu}$ is the fluid's starting viscosity and is the coefficient of pseudoplasticity (or the non-linear factor responsible for the fluid's non-Newtonian effects). For $\kappa = 0$, the model works for Newtonian lubricants, for $\kappa < 0$, dilatant lubricants, and for $\kappa > 0$, pseudoplastic lubricants.

Equation of continuity is

$$\frac{1}{\bar{r}}\frac{\partial}{\partial\bar{r}}(\bar{r}\bar{u}) + \frac{\partial\bar{w}}{\partial\bar{z}} = 0 \quad (3)$$

Momentum equation is

$$\rho\left(\bar{u}\frac{\partial\bar{u}}{\partial\bar{r}}+\bar{w}\frac{\partial\bar{u}}{\partial\bar{z}}\right)=-\frac{\partial\bar{p}}{\partial\bar{r}}-\frac{1}{\bar{r}}\frac{\partial}{\partial\bar{r}}(\bar{r}\bar{\tau}_{\bar{r}\bar{r}})-\frac{\partial(\bar{\tau}_{\bar{r}\bar{z}})}{\partial\bar{z}}-\rho g \quad (4)$$

$$\rho\left(\bar{u}\frac{\partial\bar{w}}{\partial\bar{r}}+\bar{w}\frac{\partial\bar{w}}{\partial\bar{z}}\right)-\frac{\partial\bar{p}}{\partial\bar{z}}+\frac{1}{\bar{r}}\frac{\partial}{\partial\bar{r}}(\bar{r}\bar{\tau}_{\bar{r}\bar{z}})+\frac{\partial(\bar{\tau}_{\bar{z}\bar{z}})}{\partial\bar{z}}+\rho g \quad (5)$$

Energy equation is

$$\rho c_p\left(\bar{u}\frac{\partial\bar{\theta}}{\partial\bar{r}}+\bar{w}\frac{\partial\bar{\theta}}{\partial\bar{z}}\right)=K\left(\frac{\partial^2\bar{\theta}}{\partial\bar{r}^2}+\frac{1}{\bar{r}}\frac{\partial\bar{\theta}}{\partial\bar{r}}+\frac{\partial^2\bar{\theta}}{\partial\bar{z}^2}\right)+\bar{\tau}_{\bar{r}\bar{r}}\frac{\partial\bar{u}}{\partial\bar{r}}+\bar{\tau}_{\bar{r}\bar{z}}\frac{\partial\bar{w}}{\partial\bar{r}}+\bar{\tau}_{\bar{z}\bar{r}}\frac{\partial\bar{u}}{\partial\bar{z}}+\bar{\tau}_{\bar{z}\bar{z}}\frac{\partial\bar{w}}{\partial\bar{z}} \quad (6)$$

Using the new form: $\tilde{z}=\bar{z}-c\bar{t}$ (7)

Parameters with no dimensions are introduced

$$z=\frac{\tilde{z}}{\lambda},h=\frac{\bar{h}}{b},\bar{t}=\frac{\lambda t}{c},\phi=\frac{\bar{a}}{b},\alpha=\frac{b}{\lambda},R_e=\frac{\rho cb}{\mu},E_1=\frac{-\sigma b^3}{\lambda^3\mu},E_2=\frac{mb^3}{\lambda^3},E_3=\frac{C'b^3}{\lambda^2\mu},\bar{w}=\frac{w}{c},\bar{u}=\frac{ubc}{\lambda},\bar{\theta}=\frac{\theta}{c},B_r=\frac{\kappa c^2}{\theta_0 b^2},Pr=\frac{\mu C_p}{\rho g},\bar{\tau}_{\bar{r}\bar{z}}=\frac{\tau_{rz}}{\mu\left(\frac{c}{b}\right)^4},\bar{p}=\frac{pb^5}{\lambda c^4\mu},\bar{r}=\frac{r}{b} \quad (8)$$

In their most basic form, the equations that regulate motion and energy can be expressed as (the lubrication method).

$$\frac{\partial u}{\partial r}+\frac{u}{r}+\frac{\partial w}{\partial z}=0 \quad (9)$$

$$R_e\alpha^3\left(u\frac{\partial u}{\partial r}+w\frac{\partial u}{\partial z}\right)=-\frac{\partial p}{\partial r}+\alpha^2\frac{\partial\tau_{rz}}{\partial z}+\frac{\alpha}{r}\frac{\partial(r\tau_{rr})}{\partial r}-\frac{\rho g b^5}{\mu c^4} \quad (10)$$

$$R_e\alpha\left(u\frac{\partial w}{\partial r}+w\frac{\partial w}{\partial z}\right)=-\frac{\partial p}{\partial z}+\frac{1}{r}\frac{\partial(r\tau_{rz})}{\partial r}+\alpha\frac{\partial(r\tau_{zz})}{\partial z}+\frac{\rho g b^5}{\mu c^4} \quad (11)$$

$$R_e\alpha Pr\left(u\frac{\partial\theta}{\partial r}+w\frac{\partial\theta}{\partial z}\right)=\frac{1}{r}\frac{\partial\theta}{\partial r}+\frac{\partial^2\theta}{\partial r^2}+\alpha^2\frac{\partial^2\theta}{\partial r^2}+Br\left(\alpha\tau_{rr}\frac{\partial u}{\partial r}+\tau_{rz}\frac{\partial w}{\partial r}+\alpha^2\tau_{zr}\frac{\partial u}{\partial z}+\alpha\tau_{zz}\frac{\partial w}{\partial r}\right) \quad (12)$$

The following is the form that Equations (10)–(12) adopt when it is assumed that the wavelength is large and the Reynolds number is low.

$$\frac{1}{r}\frac{\partial(r\tau_{rz})}{\partial r}=\frac{\partial p}{\partial z}-G \text{ , where } G=\frac{\rho g b^5}{\mu c^4} \quad (13)$$

$$\frac{dw}{dr}=\tau_{rz}+\beta{\tau_{rz}}^3 \quad (14)$$

$$\frac{1}{r}\frac{\partial\theta}{\partial r}+\frac{\partial^2\theta}{\partial r^2}+Br\,\tau_{rz}\frac{\partial w}{\partial r}=0 \text{ where } Br=Pr\,Ec \quad (15)$$

Br = Number of Brinkman's, Pr = Number of Prandtl's, and Ec = Number of Eckert's

$$w=0 \text{ at } r=h(z)=1+kz+\phi\,sin\,2\pi(z-t) \text{ where } k=\frac{m\lambda}{b} \quad (16)$$

$$\tau_{rz}=0 \text{ at } r=0 \quad (17)$$

$$\theta=0 \text{ at } r=h \quad (18)$$

$$\frac{\partial\theta}{\partial r}=0 \text{ at } r=0 \quad (19)$$

For a bendable wall, the equation of motion is

$$\Delta=p-p_0 \quad (20)$$

Where p_0 is the pressure on the outer surface of the wall caused by muscle tension, which is considered to be zero, and Δ is the operator used to characterize the motion of the stretched membrane with damping forces.

$$\Delta=-\sigma\frac{\partial^2}{\partial z^2}+m\frac{\partial^2}{\partial t^2}+C'\frac{\partial}{\partial t} \quad (21)$$

The next step after dimensionlessness is

$$\frac{\partial p}{\partial z}-\frac{1}{G}=\frac{\partial\Delta}{\partial z}=e_1\frac{\partial^3 h}{\partial z^3}+e_2\frac{\partial^3 h}{\partial z\partial t^2}+e_3\frac{\partial^2 h}{\partial z\partial t}=D(z,t) \text{ at } r=h \quad (22)$$

3. Solution Procedure:

After simplifying everything with the boundary condition (17), equation (13) can be written as

$$\tau_{rz}=\frac{1}{2}Dr \text{ where } D=\frac{\partial p}{\partial z}-\frac{1}{G} \quad (23)$$

When we plug in the value (23) into the equation (14) and apply the boundary condition (16), we get the following:

$$w=\frac{D}{4}(r^2-h^2)+\frac{\beta D^4}{80}(r^5-h^5) \quad (24)$$

By applying equations (18) and (19) to problem (15), we get the following:

$$\theta = \frac{BrD^2}{64}(h^4 - r^4) + \frac{\beta Br\, D^5}{32\times 49}(h^7 - r^7) \quad (25)$$

We can obtain this result by first solving equation (22) and then applying equation (16).

$$D(z,t) = -8\pi^3\phi\left[(e_1 + e_2)cos\ 2\pi(z-t) - e_3\frac{sin\ 2\pi(z-t)}{2\pi}\right] \quad (26)$$

According to the relationship between stream functions, velocities are defined as follows:

$$u = -\frac{1}{r}\frac{\partial\psi}{\partial z}, w = \frac{1}{r}\frac{\partial\psi}{\partial r} \text{ at } r = h \text{ and } \psi = 0 \text{ at } r = 0 \quad (27)$$

By applying equations (24) and (27), we arrive at the following:

$$\psi = -\frac{Dh^4}{16} - \frac{\beta D^4 h^7}{224} \quad (28)$$

$$u = \left[\frac{1}{16}\{D_z h^3 + 4Dh^2 h_z\} + \frac{\beta}{224}\{4h^6 D^3 D_z + 7D^4 h^5 h_z\}\right] \quad (29)$$

Where

$h_z = k + 2\pi\phi cos 2\pi(z-t)$

$D_z = 8\pi^3\phi[2\pi(e_1 + e_2)sin\ 2\pi(z-t) + e_3 cos 2\pi(z-t)]$

4. Numerical Results and Discussion-

Graph 1-Variation in velocity in r-direction with axial distance for different values of rigidity parameter

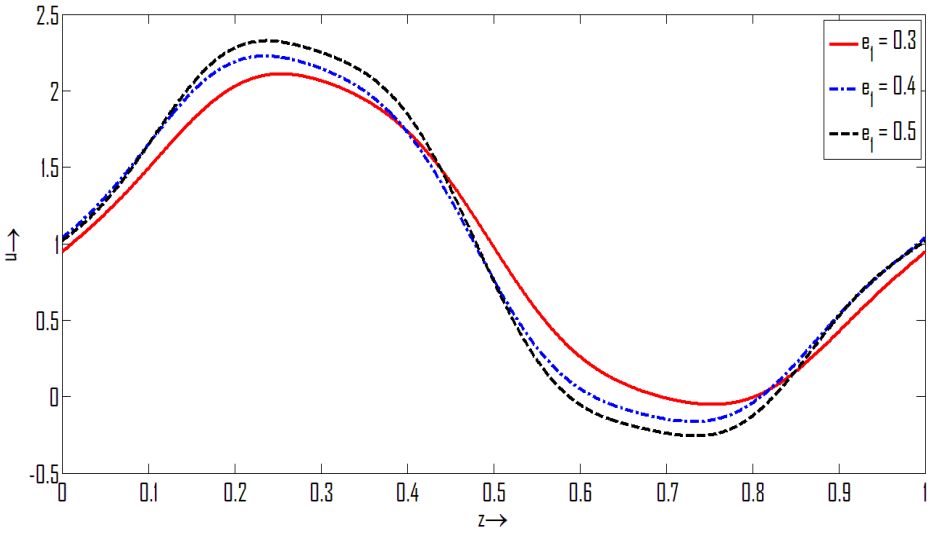

Graph 2-Variation in velocity in r-direction with axial distance for different values of stiffness parameter

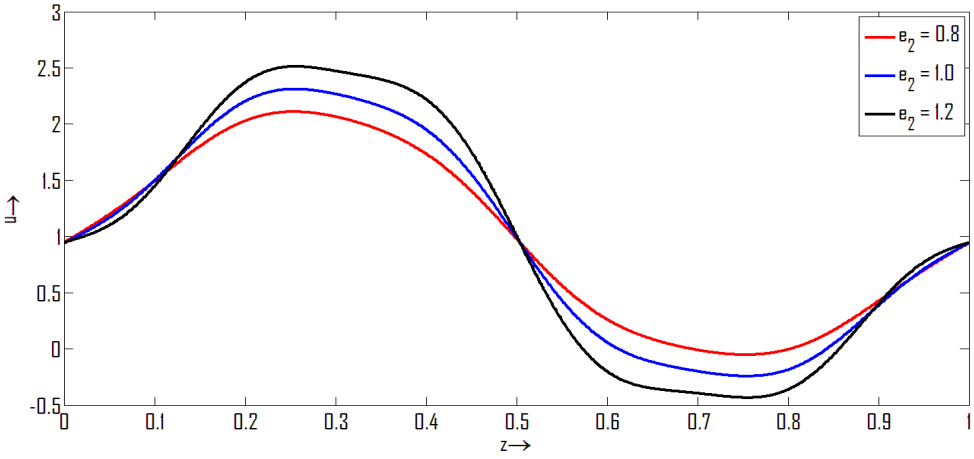

Graph 3-Variation in velocity in r-direction with axial distance for different values of viscous damping force parameter

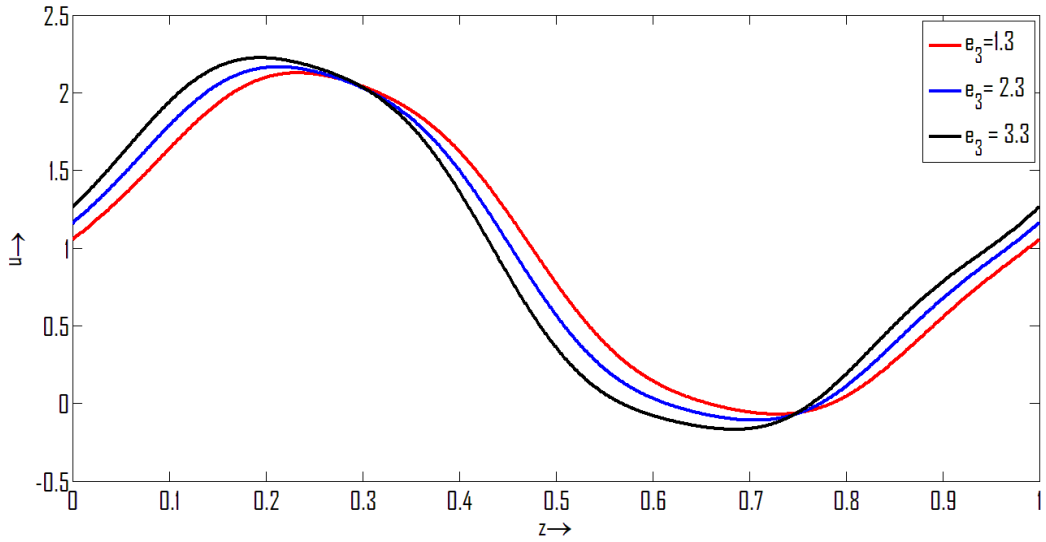

Graph 4:Variation in velocity in r-direction with axial distance and time

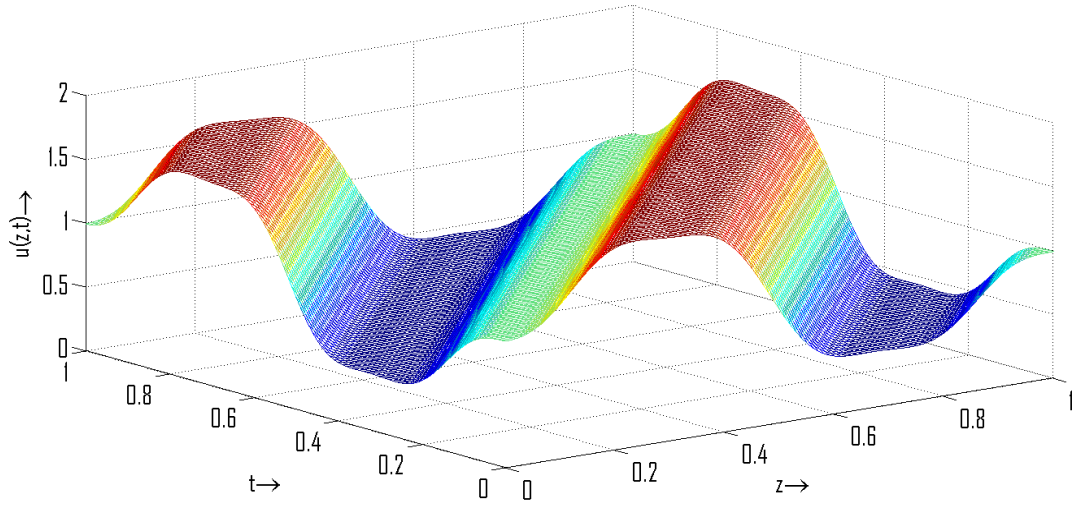

Graph 5-Variation in velocity in z-direction with radial distance for different values of rigidity parameter

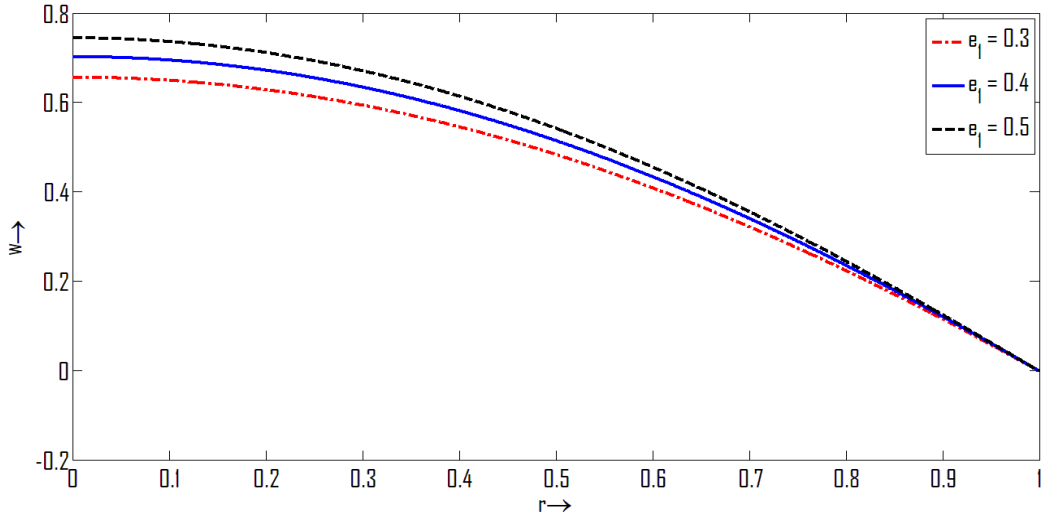

Graph 6-Variation in velocity in z-direction with radial distance for different values of stiffness paramete

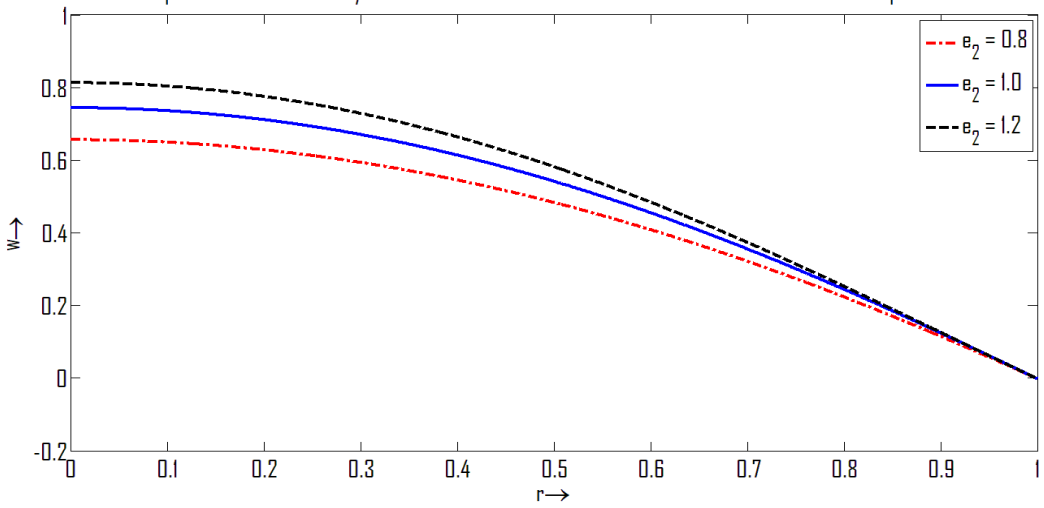

Graph 7-Variation in velocity in z-direction with radial distance for different values of viscous damping force parameter

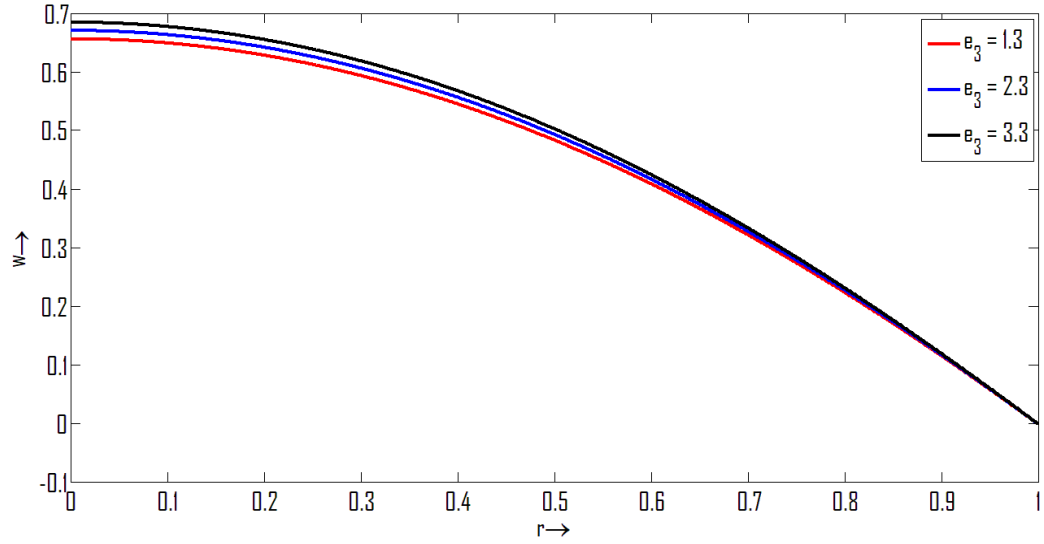

Graph 8-Variation in velocity in z-direction with axial distance for different values of wall parameters

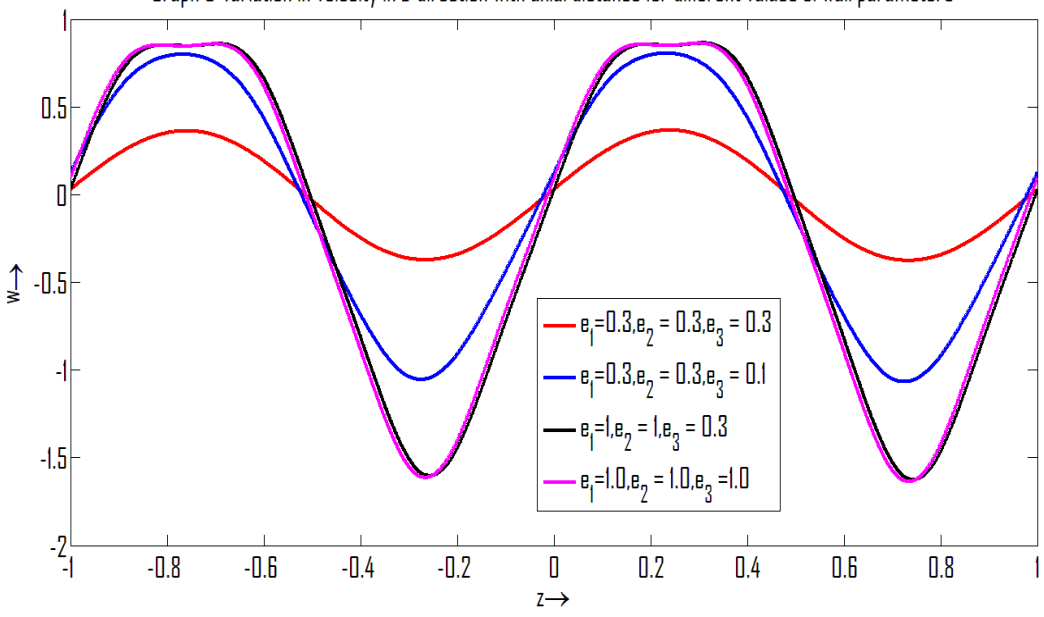

Graph 9:Variation in velocity in z-direction with axial distance and time

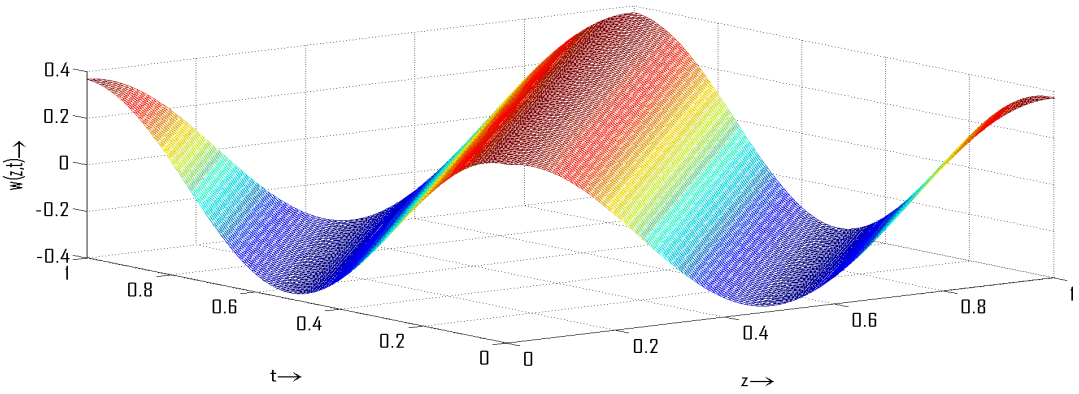

Graph 10-Variation in temperature with radial distance for different values of rigidity parameter

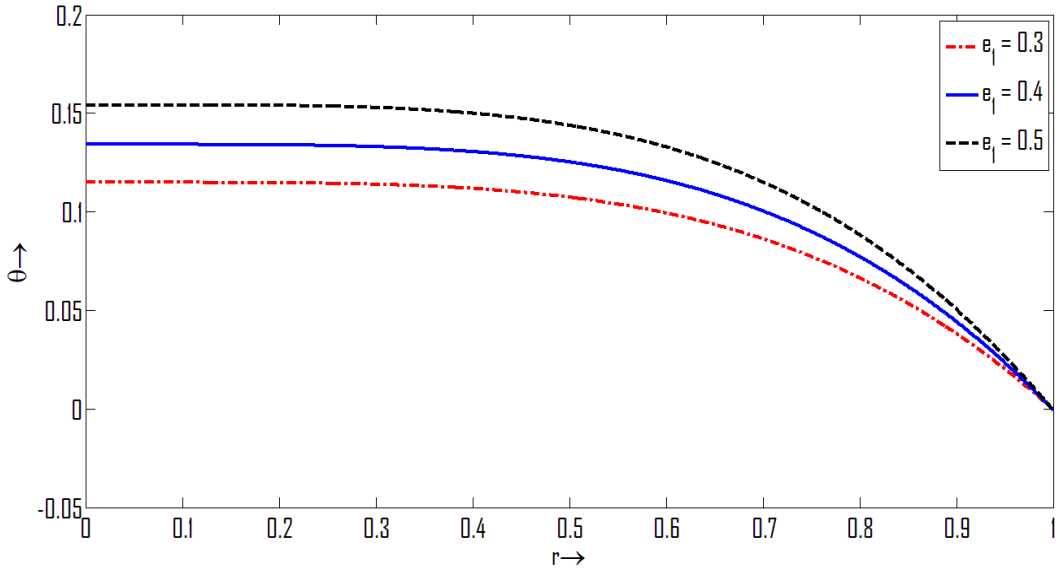

Graph 11-Variation in temperature with radial distance for different values of stiffness parameter

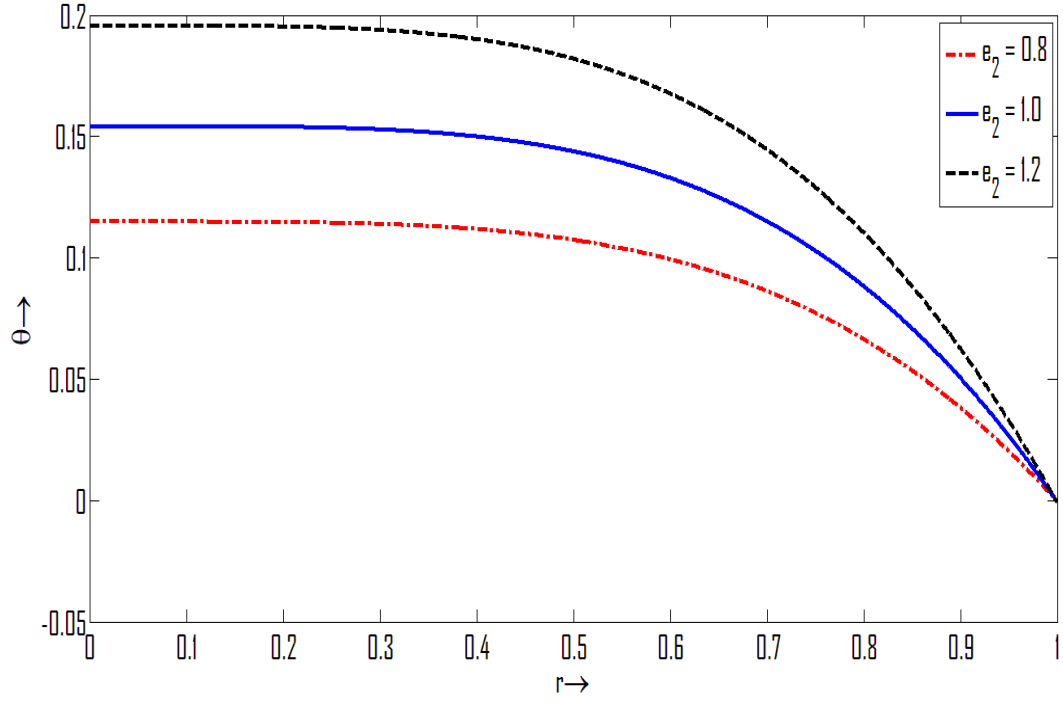

Graph 12-Variation in temperature with radial distance for different values of viscous damping force parameter

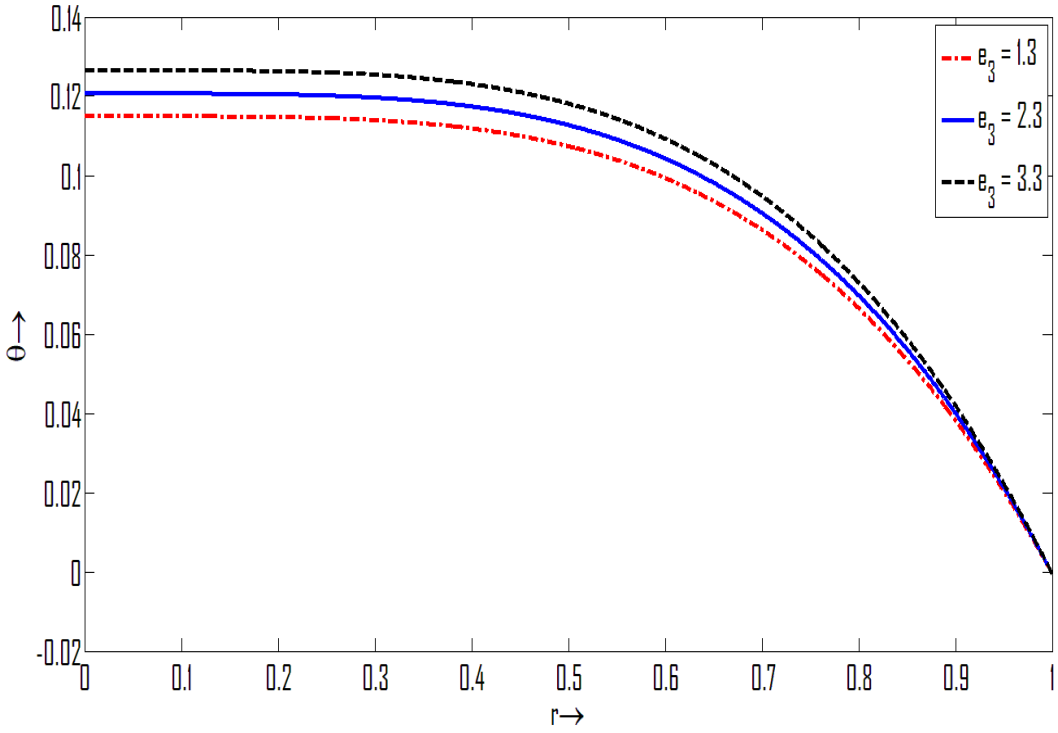

Graph 13-Variation in temperature with axial distance for different values of wall parameters

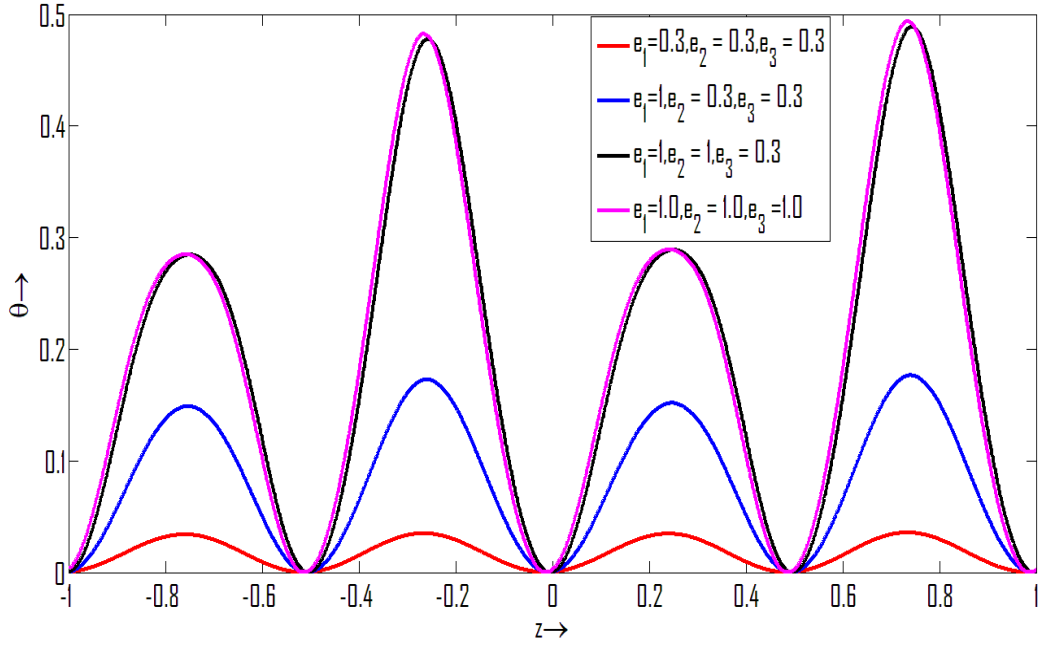

Graph 14-Variation in temperature with radial distance for different values of Brickman number

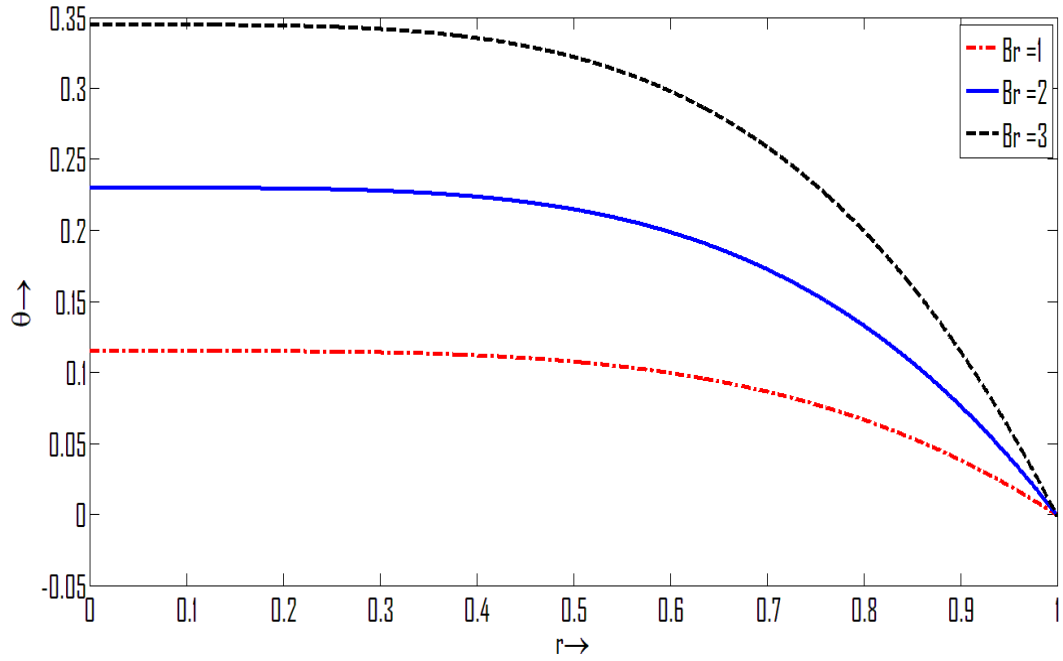

Graph 15: 3D plot of temperature with axial distance and time

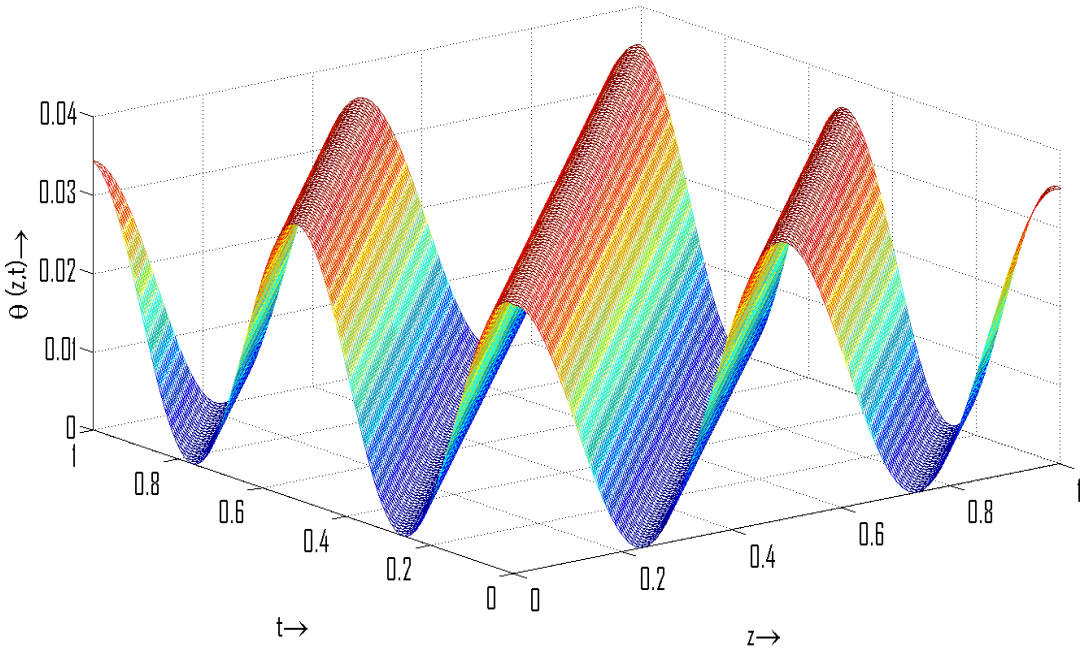

Velocity profile in r-direction(u):

Graphs 1-3 depict the relationship between the velocity in the r-direction (u) and the axial distance (z) as a function of the rigidity parameter (e_1), the stiffness parameter (e_2), and the viscous damping force parameter (e_3) , respectively. Graph (4) depicts a three-dimensional plot of u vs axial distance and time.

Velocity profile in z-direction(w):

Graphs 5–7 depict the z-direction velocity (w) as a function of radial distance (r) as a result of the influence of e_1 ,e_2 and e_3. These charts show that as the radius expands, the velocity slows down. It is also observed that the

velocity grows with the values of e_1 ,e_2 and e_3. Graph (8) shows the velocity variation for various wall qualities. Graph (9) depicts a three-dimensional plot of w vs axial distance and time.

Temperature profile (θ):

Graphs 10-12 depict the relationship between temperature and radial distance (r) as a function of e_1 ,e_2 and e_3. It can be seen from these figures that the temperature drops down dramatically with increasing radial distance. It is also observed that when e_1 ,e_2 and e_3 grow, so does the temperature. Graphs (13) and (14) show the temperature range for varying wall characteristics and Brickman numbers. These graphs show that as the Brickman number rises, so does the temperature. Figure (15) depicts a three-dimensional plot of the value of θ vs axial distance and time.

5. Concluding Remarks:

The peristaltic motion of a Rabinowitsch fluid in a tube with varying wall characteristics has been discussed in this research. The velocity and temperature distributions are solved exactly. When the parameters for rigidity and stiffness are increased, the resulting velocity profiles are steeper, while the damping force parameter yields more gradual rises in speed. When the Brickman number, rigidity parameter, stiffness parameter, and viscous damping force parameter are all raised, the resulting temperature distributions are all upward. In all cases, the Brinkman number helps to raise the liquid temperature because of its relationship to the effects of viscous dissipation. With a rising Brinkman number, the temperature profile rises. Since shear in the flow generates more heat due to friction, the fluid temperature increases at a physically bigger value of Br.

Reference:

[1] Absi, R (2018): " Revisiting the pressure-area relation for the flow in elastic tubes: application to arterial vessels", Series on Biomechanics, 32(1): 47-59.

[2] Bhattacharyya A,, Kumar R., Bahadur S., Seth G.S.(2022): "Modeling and interpretation of peristaltic transport of Eyring–Powell fluid through uniform/non-uniform channel with Joule heating and wall flexibility", Chinese Journal of Physics,80:167-182.

[3] Divya B.B, Manjunatha G., Rajashekhar C., Vaidya H., Prasad K.V. (2021): "Analysis of temperature dependent properties of a peristaltic MHD flow in a non-uniform channel: A Casson fluid model", Ain Shams Engineering Journal, 12(2): 2181-2191.

[4] Goud J.S., Reddy H.R. (2015): "Peristaltic motion of an Ellis fluid model in a vertical uniform tube with wall properties", International Journal of Civil Engineering and Technology, 9(1):847-856.

[5] Hafez N.M., Alla Abd A.M., Metwaly T.M.N. (2023): "Influences of rotation and mass and heat transfer on MHD peristaltic transport of Casson fluid through inclined plane", Alexandria Engineering Journal, 68:665-692.

[6] Hasan M.M., Samad M.A., Hossain M.M. (2020): "Peristaltic flow of non-newtonian fluid with slip effects: analytic and numerical solution", Research Journal of Mathematics and Statistics, 11(1): 1-10.

[7] Imran N., Javed M., Sohil M., Tlilli I. (2020): "Simultaneous effects of heterogeneous–homogeneous reactions in peristaltic flow comprising thermal radiation: Rabinowitsch fluid model", Journal of Materials Research and Technology, 9:3520–3529.

[8] Kameswaran P.K., Shaw S., Sibanda P., Murthy P.V.S.N. (2013): "Homogeneous–heterogeneous reactions in a nano fluid flow due to a porous stretching sheet", International Journal of Heat and Mass Transfer, 57:465–472.

[9] Nahar S., Dubey B.N., Windhab E.J. (2019): "Influence of flowing fluid property through an elastic tube on various deformations along the tube length". Physics of Fluids, 31(10):101905.

[10] Rajashekhar C.,Vaidya H., Prasad K.V.,Tlili I., Patil A., Nagathan P. (2020): "Unsteady flow of Rabinowitsch fluid peristaltic transport in a non-uniform channel with temperature-dependent properties", Alexandria Engineering Journal, 59(6):4745-4758.

[11] Saravana R., Vajravelu K., Sreenadh S. (2018): "Influence of compliant walls and heat transfer on the peristaltic transport of a rabinowitsch fluid in an inclined channel", Zeitschrift Naturforschung Teil A ,73:833–843.

[12] Singh B.K., Singh U.P. (2014): "Analysis of peristaltic flow in a tube: Rabinowitsch fluid model", International Journal of Fluids Engineering, 6(1):1-8.

[13] Singh U.P., Medhavi A., Gupta R.S., Bhatti S.S. (2017): "Analysis of peristaltic transport of non-Newtonian fluids through non uniform tubes: rabinowitsch fluid model", Zeitschrift für Naturforschung A, 72:601–608.

[14] Yasodhara G., Sreenadh S., Sumanlatha B., Srinivas A.N.S (2020): "Axisymmetric peristaltic flow of a non-newtonian fluid in a channel with elastic walls", Mathematical Modelling of Engineering Problems, 7(2): 315-323.